energies

Article

Sedimentary Characteristics of Lacustrine Beach-Bars and Their Formation in the Paleogene Weixinan Sag of Beibuwan Basin, Northern South China Sea

Jie He [1,*], Hua Wang [2], Tao Jiang [1], Entao Liu [1], Si Chen [2] and Ping Jiang [3]

1 College of Marine Science and Technology, China University of Geosciences, Wuhan 430074, China; taojiang@cug.edu.cn (T.J.); liuentao@cug.edu.cn (E.L.)
2 School of Earth Resources, China University of Geosciences, Wuhan 430074, China; wanghua@cug.edu.cn (H.W.); sichen720@hotmail.com (S.C.)
3 Zhanjiang Branch Company, China National Offshore Oil Corporation, Zhanjiang 524057, China; jiangp@cnooc.com.cn
* Correspondence: jiehe19920402@163.com

Abstract: Beach-bar reservoirs have been promising hydrocarbon-bearing exploration advances in the Beibuwan Basin, especially in the WZ12-2 area within the Weixinan sag. The sedimentary characteristics, distribution and formation mechanisms of beach-bar sand bodies in Mbr2 (Member 2) of the Paleogene Liushagang Fm. in the WZ12-2 area within the Weixinan sag were analyzed based on well-log, seismic and core data on thin section and heavy mineral data. Mbr2 in the WZ12-2 area comprises a third-order sequence, which consists of three systems tracts (lowstand systems tract, transgressive systems tract and a locally developed highstand systems tract). Thick beach-bar sand bodies are developed in the WZ12-2 area during the lowstand systems tract stage. The formation of sandy beach-bar sand bodies can be divided into five stages. By integrating lithology, mineral composition, sedimentary structures and geophysical characteristics, it can be concluded that the beach-bar sand bodies in the study area were controlled by paleotopography, hydrodynamic environment, sediment provenance and lake-level variation. The gentle slope of the Qixi uplift and relatively stable passive tectonic background during the deposition of Mbr2 of the Liushagang Fm. laid a solid paleogeomorphological foundation for beach-bar deposition. Strong hydrodynamic forces and shallow water further contributed to beach-bar sand bodies formation. In addition, the sands in the fan delta in the northwestern part of the area served as point provenance and the deposits in the southeast acted as linear provenance in providing sediments to the beach-bars. High-frequency variations of the lake level drove vertical stacking of the beach-bar sand bodies and considerable lateral extension over a large area. The sedimentary characteristics and formation mechanism of lacustrine beach-bars in this study may provide a reference for hydrocarbon exploration in other similar basins in the world.

Keywords: beach-bars; Beibuwan Basin; Weixinan sag; sedimentary characteristics; formation mechanism

check for updates

Citation: He, J.; Wang, H.; Jiang, T.; Liu, E.; Chen, S.; Jiang, P. Sedimentary Characteristics of Lacustrine Beach-Bars and Their Formation in the Paleogene Weixinan Sag of Beibuwan Basin, Northern South China Sea. *Energies* **2022**, *15*, 3391. https://doi.org/10.3390/en15093391

Academic Editor: Reza Rezaee

Received: 23 March 2022
Accepted: 29 April 2022
Published: 6 May 2022

1. Introduction

Beach-bar refers to the beach and bar sand bodies in lacustrine or marine basins with a shallow water environment [1–6]. In the gently sloping area of a rifted lacustrine basin, beach-bar sand bodies tend to develop in shallow littoral lakes [4,7,8]. Beach-bars can usually be subdivided into bioclastic and terrigenous clastic types [2,4,9]. Bioclastic beach-bars usually develop in quiet and clear lake water under warm and humid condition with carbonate provenance [10]. Terrigenous clastic beach-bar sand bodies form from the redeposition and reworking of deltas and other related near-shore sedimentary systems in a shallow water environment under the effects of fluctuations in energy conditions from coastal currents and waves [11–14]. Generally, lacustrine beach-bars are mostly characterized by thin interbedded sand bodies mainly composed of fine sandstone and siltstone with restricted distributions [2].

The Beibuwan Basin, which is an extensional Cenozoic sedimentary basin, is characterized by lacustrine deposits in Paleogene and littoral-neritic sea sediments in Neogene-Quaternary [15]. It is a productive basin in the northern South China Sea (Figure 1A) [15,16]. The northern part of the Beibuwan Basin has been proven to be a prospective area for further petroleum exploration [17–20]. Recently, important breakthroughs in the Weixinan sag have been achieved (Figure 1B) [21]. The Southeast Slope Belt is one of the largest hydrocarbon-producing targets in the Weixinan sag (Figure 1C) [19]. Among the oil fields in the Southeast Slope Belt, the WZ12 oil field produces abundant oil and gas. The beach-bars developed in the WZ12-2 area of Mbr2 of the Liushagang Fm. have now become important exploration targets in the Beibuwan Basin [20,22,23]. A beach-bar sand reservoir has grain size dominated by fine sand and sand, good sorting, well-developed primary and secondary porosity, and relatively high permeability. Beach-bar sand bodies change frequently on a lateral scale, easily forming lithologic lenticular traps and sandstone pinch-out traps [4,14,24]. The dark mudstone at the bottom provides hydrocarbons for the beach-bar reservoirs in the Mbr2 stage of Liushagang Formation [16]. The overlying thick dark mudstone can act as a superior caprock for beach-bar reservoirs underneath [25–27]. With superior hydrocarbon generation and sealing conditions, beach-bar sand bodies in the WZ12-2 area are evaluated as prospective exploration targets. During the depositional period of Mbr2 in the Weixinan sag, especially during the lowstand systems tract (LST) stage, beach-bar sand bodies formed on a large scale [23,28]. In the past few years, considerable attention has been given to the petroleum source of WZ12 oils in Mbr2 of the Liushagang Fm. in the Weixinan sag [16,17,21,29]. However, studies on the reservoir are scarce.

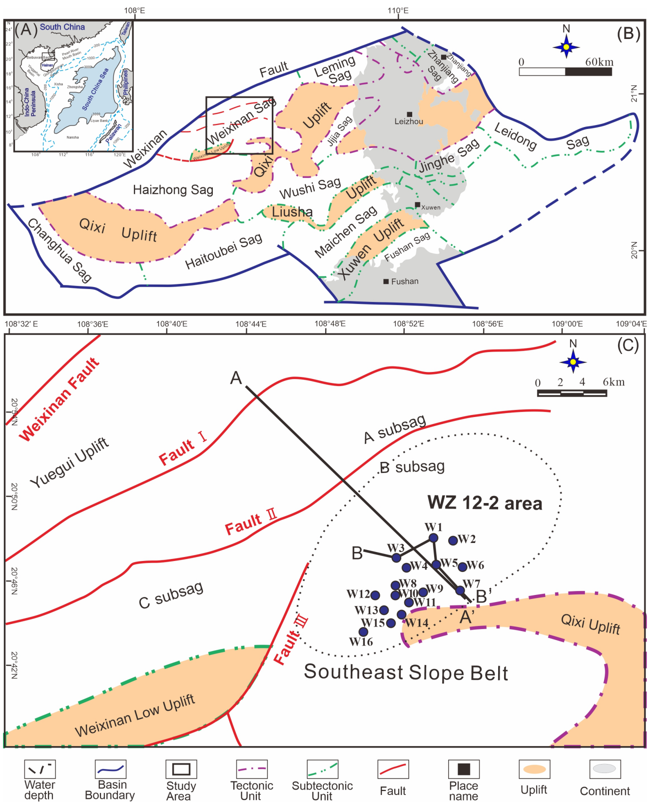

Figure 1. (**A**) Location of sedimentary basins in the South China Sea. The black box indicates the location of Figure 1B; (**B**) simplified geological map of the Beibuwan Basin [16,20]. The Weixinan sag was located in the northwestern Beibuwan Basin. The black box refer to the study area in Figure 1C; (**C**) simplified geological map of the Weixinan sag. The black line AA′ and BB′ mark the locations of seismic section and sequence stratigraphic correlation sections in Figures 3 and 9, respectively.

In this regard, good hydrocarbon source rocks and thick top seals are present in the Mbr2 stage in the WZ 12-2 area. Further steps are to find superior hydrocarbon "container"—reservoirs, to form potential source-reservoir-cap assemblages, which are of great significance to hydrocarbon exploration. In this study, the sedimentary characteristics, i.e., lithology, mineral composition, sedimentary structures and geophysical characteristics of the beach-bar sand bodies, are analyzed concretely to investigate the formation mechanism, on the basis of thin section, heavy mineral, core, well logging and 3D seismic data. This study can be useful for further hydrocarbon prospecting and exploration in the Weixinan sag and has great significance for further application to lacustrine rift basins with similar backgrounds in the world.

2. Geological Background

The Beibuwan Basin has an area of approximately 1.9×10^4 km^2 onshore and 1.6×10^4 km^2 offshore [15,30]. The development of the Beibuwan Basin includes two main stages: the Paleogene syn-rifting stage (65–23 Ma) and the post-rifting stage (23 Ma to present) (Figure 2) [20,31]. The Weixinan sag located in the northwestern Beibuwan Basin is a half-graben rift lake basin bounded by the Qixi uplift to the southeast, the Weixinan fault to the northwest, and the Haizhong sag and Weixinan low uplift to the southwest (Figure 1B) [15].

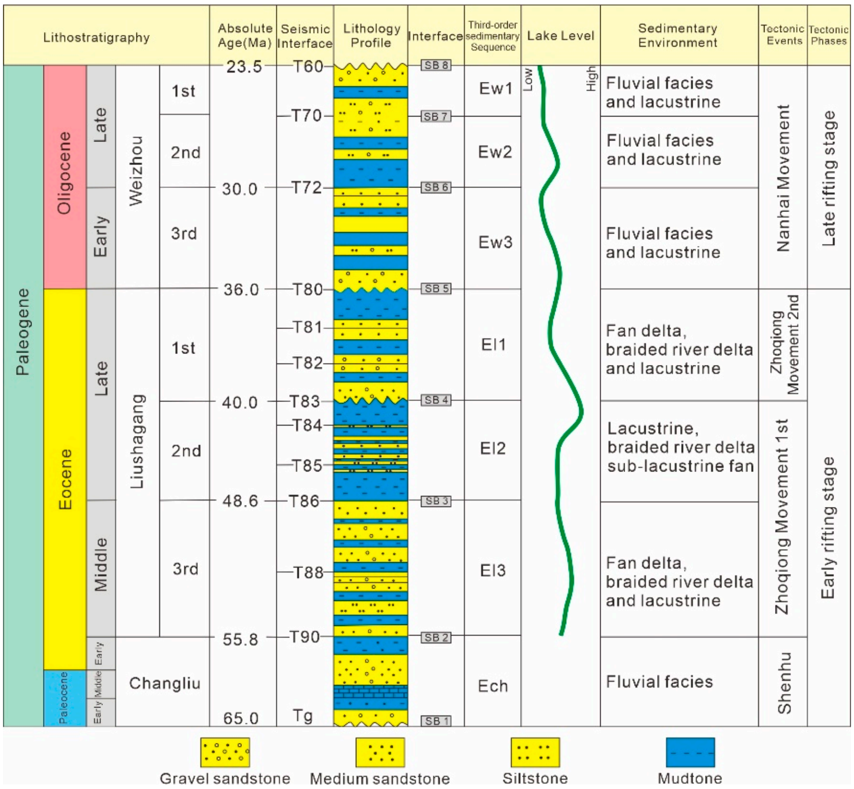

Figure 2. The Paleogene sedimentary sequence and stratigraphic framework of the Beibuwan Basin [31].

The A, B and C sub-sags formed in response to three extensional events in Paleocene, Eocene and middle-late Oligocene (Figure 1C). The three growth normal faults (Fault I, Fault II and Fault III) in the NE-SW direction have large fault throws up to several thousand meters and long extents with lengths of more than 40 km (Figure 3) [16]. In the Paleogene, the depositional environments in the Weixinan sag were dominated by fan delta, shore-shallow lake delta and lacustrine facies [31].

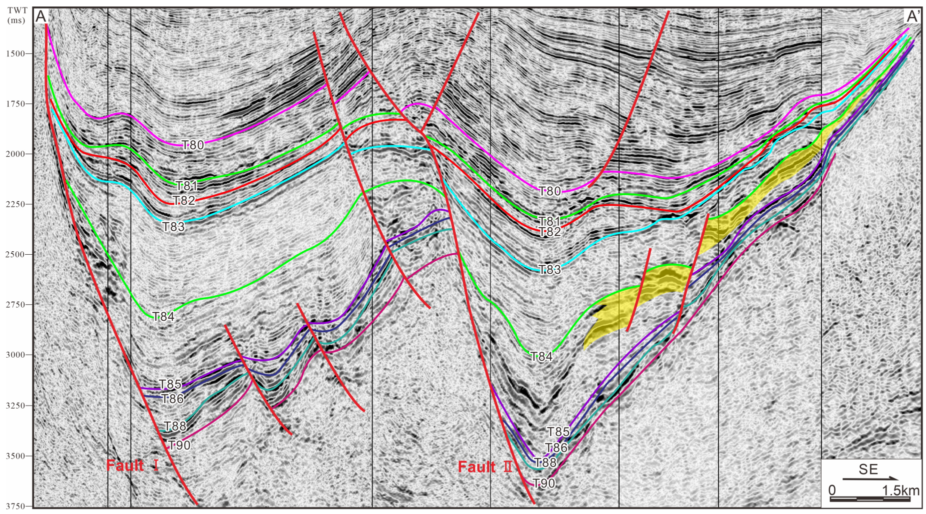

Figure 3. Seismic section (northwest to southeast) across the Weixinan sag showing the sequence boundaries, stratigraphic units and major faults. The targeted Mbr2 of the Liushagang Fm. is from T85 to T84 reflectance surface. The light yellow color in the figure refers to the beach-bar deposition.

Based on logging core, drilling, 3D seismic, paleontological and geochemical data, the stratigraphy of the Paleogene in the Weixinan depression has been reconstructed. The Paleogene sediments in the Weixinan depression are composed of the Changliu Fm., Liushagang Fm. and Weizhou Fm. and seven third-order sequences (Ech, El3, El2, El1, Ew3, Ew2 and Ew1) from bottom to top [31]. As the primary and crucial oil and gas-bearing reservoir, the Liushagang Fm. (including Mbr3, Mbr2, and Mbr1) is the main depositional unit in the Weixinan sag (Figure 2). The main sedimentary environments in Mbr3 and Mbr1 are shallow lacustrine and shore-shallow deltas, and lacustrine environments prevailed during Mbr2 deposition [20]. The beach-bars formed in Mbr2 of the Liushagang Fm. in WZ12-2 area of the Weixinan sag.

3. Materials and Methods

This study integrated logging, core and 3D seismic data with thin section, scanning electron microscopy (SEM) and heavy mineral analyses. Wireline log data from 16 wells and more than 2000 km^2 3D seismic data were analyzed. Approximately 40 m of cores from 3 wells were studied. This study also analyzed heavy minerals from 16 wells, grain-size analysis from 51 samples, and porosity and permeability data from 75 samples. All the data were acquired from the CNOOC Zhanjiang Branch Company.

Depositional systems tracts and sequences were first recognized in the WZ12-2 area of the Weixinan sag, mainly on the basis of termination patterns and seismic reflections [32]. They were further confined by core data and wireline logs along the main seismic sections. Depositional and stratigraphic cross-sections throughout the Weixinan sag were established to depict the lateral and vertical distributions of the lacustrine beach-bar facies. The logging, core, grain-size, porosity, permeability and SEM data were used to identify the sedimentary characteristics of the beach-bars. The controlling factors of lacustrine beach-bar formation in the study area were investigated by the reconstruction of paleotopography, sediment source systems and lake levels. Then, a distribution model of lacustrine beach-bar sand bodies was established within the Weixinan sag.

On the basis of well log, drilling core and 3D seismic data, Mbr2 in the Weixinan sag was identified as a third-order sequence, including a lowstand systems tract (LST) and a transgressive systems tract (TST). The highstand systems tract (HST) was not well developed and seen only as thin layers in several wells. In seismic sections, the T83 reflector marking the top sequence boundary separates Mbr1 and Mbr2. The bottom sequence boundary is marked by the T86 reflector that divides Mbr2 and Mbr3. T83 and T86 are regional unconformable surfaces along the basin edges. On seismic profiles, onlap and erosional truncation terminations are observed on the T83 and T86 surfaces (Figure 3).

Scanning electron microscopy (SEM) was conducted with TESCAN-VEGA equipped with an SDD detector, pulse processor and Esprit software workstation. Samples for heavy mineral analysis were first processed to remove the weathered rims, carbonate materials and clay minerals. Then the 63–125 µm fraction were separated by magnetic and electrostatic filters. About 700–1000 heavy mineral grains were identified under the binocular microscope for each sample. The porosity and permeability were measured following Boyle's and Darcy's laws, respectively, by using 2.5 cm diameter cylinders drilled from the cores.

4. Results

4.1. Sedimentary Characteristics

4.1.1. Lithology

The lithologies of lacustrine beach-bar sands are usually composed of siltstone, fine-grained sandstone and pelitic siltstone [4,33]. In the WZ12-2 area, the sandstones of the beach-bars are mainly grey and greyish-brown siltstone and fine- to medium-grained sandstone (Figure 4). The logging and core data indicate that there are few layers of sandstone but that the single layer thickness is large, usually thicker than 3 m. An individual sandy bar layer in the LST can be thicker than 10 m and is interbedded with thin mudstones, showing coarsening trends in the vertical direction. The sandy bar sediments in well W5 are dominated by sand, which makes up 92% of the total content (Figure 4).

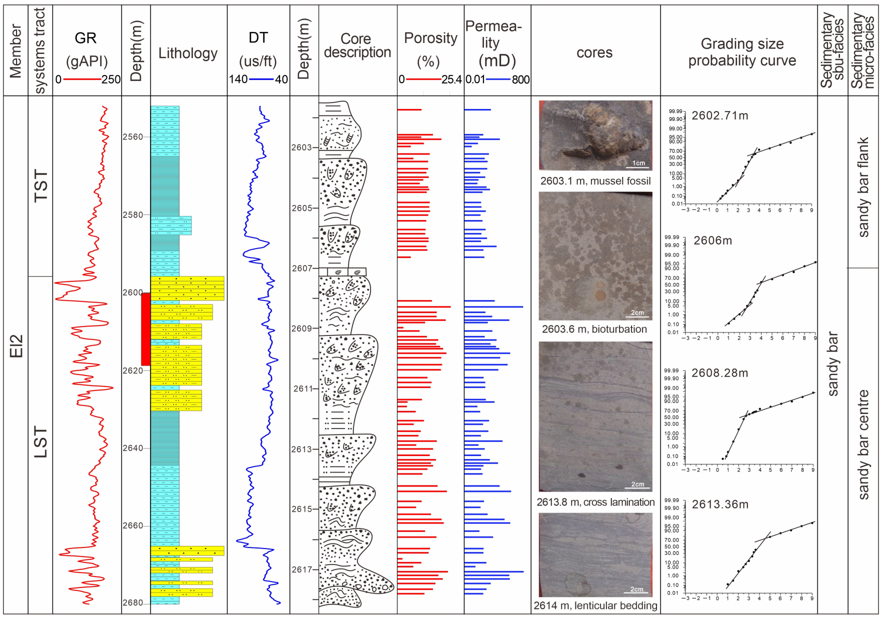

Figure 4. Single well integrated diagram of the beach-bar sand bodies of well W5 in the Weixinan sag. The red rectangle emphasized on the left logging lithologic column refers to the core description in the right.

4.1.2. Mineral Composition

Quartz is the most frequent and abundant mineral in beach-bar sandstones. The quartz content in the WZ12-2 beach-bar reservoirs ranges between 52% and 77%, with an average of 67% (Figure 5A,B). Feldspars in the study area include potassium feldspar and plagioclase (Figure 5H,L), and the percentage of plagioclase is higher than that of potassium feldspar. The average feldspar content is 10%. The lithic fragment content is approximately 5%, and fragments are predominantly argillaceous clasts. The detrital compositions of beach-bar sandstones are mainly litho-quartzose and feldspatho-litho-quartzose sandstones, with subordinate feldspatho-quartzose sandstones and minor litho-feldspatho-quartzose, quartzo-lithic and quartzose sandstones (Figure 6) [34]. The compositional maturity of the beach-bar sand bodies is high (average 2.2), ranging from 1.1 to 3.7. Thin section observations indicate that there are intraclasts of partly dissolved ooids and muddy and silty limestones with plastic deformation in sandstones of the beach-bar (Figure 5C–E,H). The carbonate sediments are redeposited in shallow lacustrine environments after reworking by waves. The intraclasts, which consist of freshly deposited and loosely compacted carbonate sediments, suggest that the carbonate sediments originated internally from the basin. Both the high compositional maturity and the occurrence of oolitic particles with thin crusts reflect the high frequency oscillation of lake water and long-term reworking of the sediments.

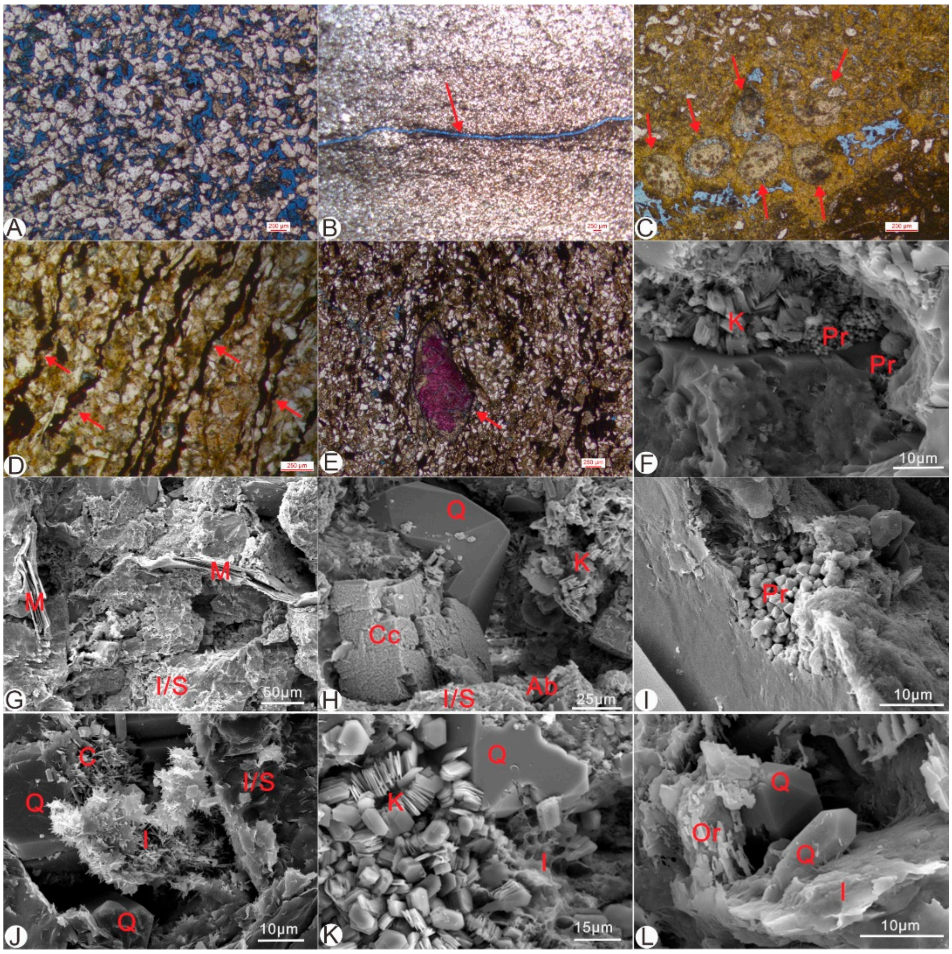

Figure 5. Thin section and SEM images providing information about the mineral composition of beach-bar sandstones in Weixinan sag. (**A**) Well W5, 2610.20 m, high content of quartz and porosity (polarized light). (**B**) Well W5, 2604.38 m, micro-fractures in beach-bar reservoir (polarized light). (**C**) Well W5, 2603.20 m, carbonate oolites (polarized light). (**D**) Well W5, 2612.56 m, black banded carbonaceous fragments (polarized light). (**E**) Well W5, 2605.71 m, carbonaceous fragments and dissolution of detrital grains (polarized light). (**F**) Well W6, 2435.90 m, booklet-like kaolinite and pyrite framboids (SEM). (**G**) Well W1, 3327.04 m, deformation of mica and hairy illite-smectite mixed layers (SEM). (**H**) Well W13, 2266.80 m, authigenic carbonate cement, quartz, booklet-like kaolinite and partly dissolved albite (SEM). (**I**) Well W1, 3331.35 m, octahedral pyrites (SEM). (**J**) Well W1, 3334.50 m, fibrous illite, quartz and flaky illite-smectite mixed layers (SEM). (**K**) Well W12, 2755.82 m, booklet-like kaolinite, quartz and honeycombed illite (SEM). (**L**) Well W12, 2699.52 m, quartz and partly dissolved orthoclase (SEM). Ab—albite, Cc—carbonate cement, I—illite, I/S-illite and smectite mixed layer, K—kaolinite, M—mica, Or—orthoclase. Pr—pyrite, Q—quartz.

Microscopic data show that quartz is common in beach-bar sand bodies (Figure 5H,J–L). Orthoclase and albite are partly dissolved (Figure 5H,L). Under SEM, micas have a flaky morphology and are deformed by compaction (Figure 5G). Carbonate cements principally include calcite, dolomite and ankerite, and the most abundant type is calcite. The calcite cements developed in the WZ 12-2 beach-bar sandstones are rhombic crystals filling in intergranular pores (Figure 5E,H). Pyrite is present as framboids (Figure 5F) and octahedrons (Figure 5I) in beach-bar sandstones. Clay minerals in the WZ 12-2 beach-bar sandstone reservoirs are mainly authigenic clay minerals and matrix materials. The clay minerals observed in beach-bar reservoirs are kaolinite (Figure 5F,H,K), illite (Figure 5J–L), illite-smectite mixed layer minerals (Figure 5G,H,J) and chlorite (Figure 5J). Kaolinite forms as pore-filling cement, presenting booklet or vermicular pseudohexagonal morphologies. Illite occurs with fibrous and sheet textures. The illite-smectite mixed-layer clays have honeycomb and flake textures. Chlorite grows as rims along detrital grain surfaces.

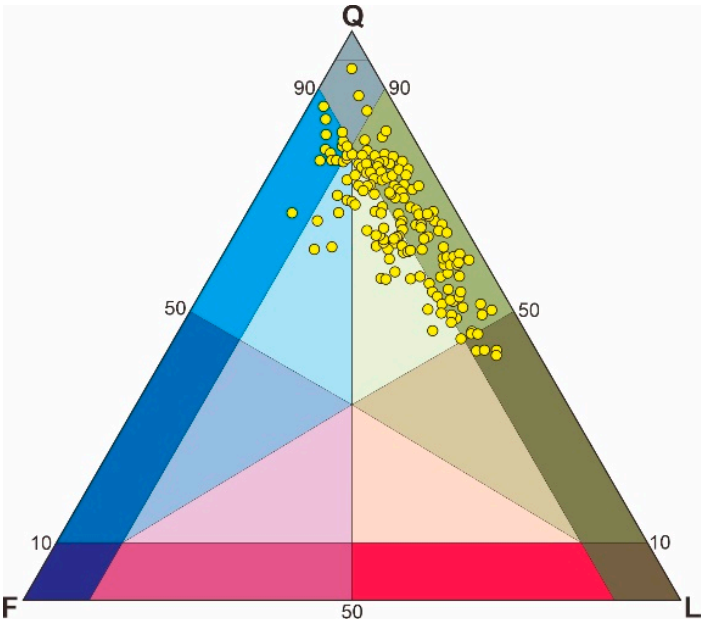

Figure 6. Detrital composition triangular diagram of the beach-bar sandstones in the Weixinan sag [34]. The detrital composition of beach-bar sandstones are mainly litho-quartzose and feldspatho-litho-quartzose sandstones.

Heavy minerals in the study area are mainly zircon, tourmaline, rutile, garnet, hematite, limonite, magnetite and titanomorphite. The zircon contents are between 0.2% and 20%, with an average value of 5.2%. The percentage of tourmaline varies from 0.2% to 27.6%, and the average value is 4.5%. Rutile has an average content of 0.82%, ranging from 0.2% to 2.9%. The garnet content varies from 0.2% to 19.4% with an average of 3.2%. Hematite and limonite have the highest contents. They account for an average of 61.2% of the total heavy minerals, varying from 1% to 97.8%. Magnetite and titanomorphite have average values of 5.7% and 19.9%, fluctuating between 0 and 30.8%, and between 0.2% and 91.6%, respectively (Figure 7).

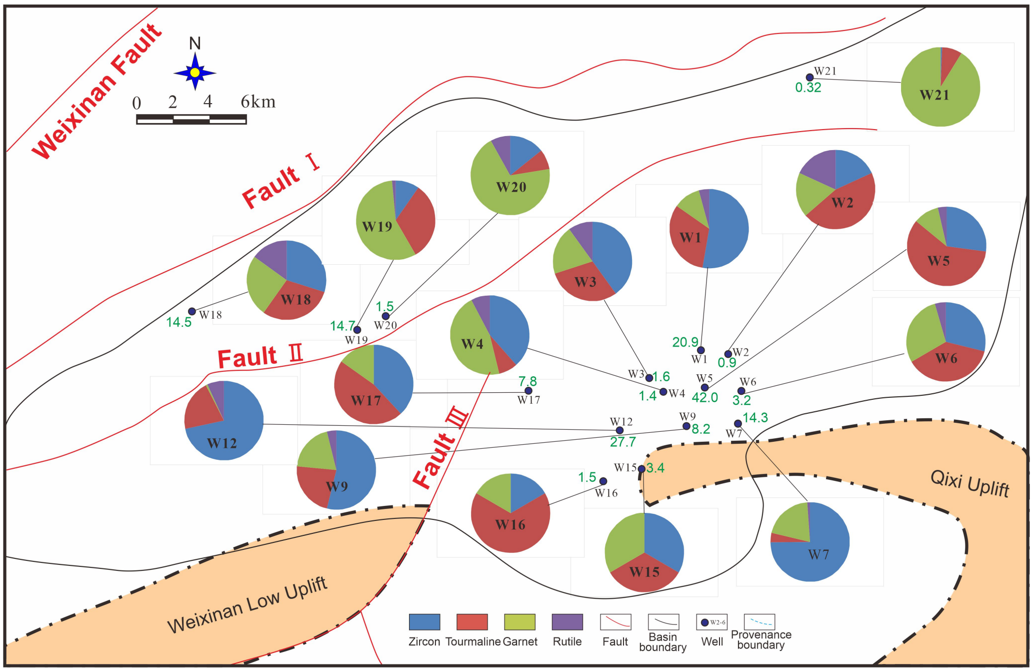

Figure 7. The pie chart of heavy mineral assemblage (zircon + tourmaline + garnet + rutile) percentage and ZTR index of the Mbr2 in the Weixinan sag. The numbers beside the wells are the ZTR values of the wells.

4.1.3. Sedimentary Structures

The sedimentary structures observed in the WZ12-2 beach-bar sandstones have obvious characteristics implying a fluctuating hydrodynamic environment in the lake. Combined-flow ripple cross-lamination or current ripple with lenticular bedding and claystone drapes are observed in the cores (Figure 4). The sandstone beds are massive or horizontally stratified and covered by combined-flow (or current) and interlaminated and interbedded with laminated siltstones or mudstones. These sedimentary structures suggest scouring, reworking and multi-directional flows by waves during deposition [2,35,36]. Teichichnus and fugichnia bioturbation structures are common with various morphologies under different depositional hydrodynamic energies. The presence of mussel bivalve fossils indicates shallow water depths during beach-bar deposition.

4.1.4. Geophysical Characteristics

As the sand bodies of sandy beach-bars in the WZ12-2 area are thick and interbedded with muds, the wireline logging curves are dagger-like or broad-amplitude tooth-shaped boxes and funnel-like shapes with relatively high amplitude (Figure 8). The beach-bars in the WZ12-2 area formed between regional unconformity interface T84 and fourth-order sequence interface T85. The beach-bar reservoirs deposited during the Mbr2 stage have distinctive seismic reflection characteristics with two strong and continuous seismic reflectors, which are also the top interfaces of beach-bar sand bodies. Two obvious inverse superimposed cycles are observed in the wireline logs of wells W1 and W5. The sand thickness increases upward in each cycle, and the mud layers become thinner, indicating that the base level was falling when the beach-bars formed [2]. The grain-size cumulative probability curves show that the core samples of beach-bar sands from well W5 formed mainly from saltating and suspended particles. The saltation types correspond to 60–70% of the whole grain-size curve. A saltation-type curve section is composed of 2–3 segments. The intersection point between the suspended and saltation types is at 3–4Φ (Figure 4). The porosity of well W5 ranges from 2.32% to 23.4% with an average of 13.7%. The permeability of well W5 has an average value of 11.38 mD, varying from 0.01 mD to 357 mD.

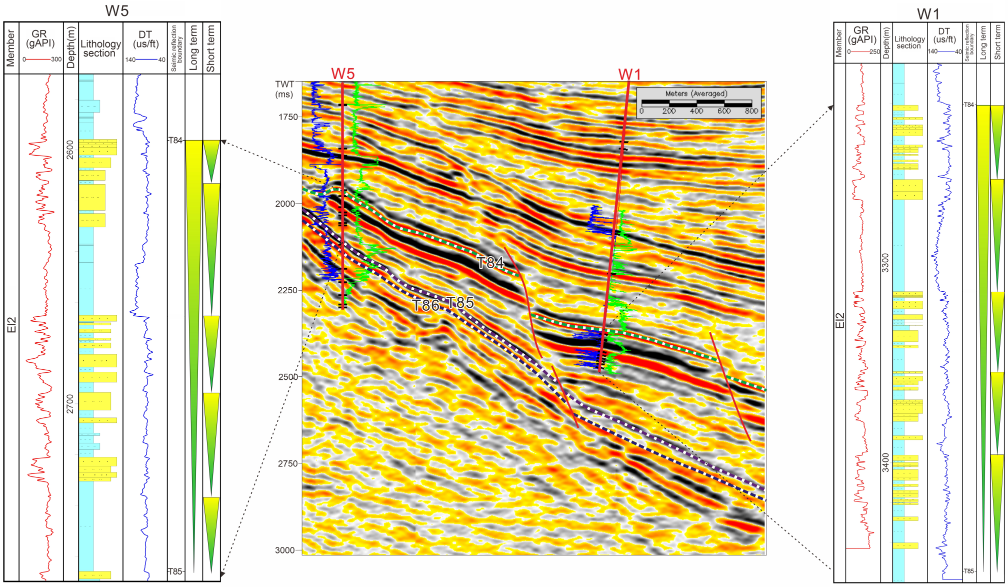

Figure 8. Base level division combined with seismic section of beach-bar sand bodies of Mbr2 stage in the Weixinan sag. The beach-bar sand bodies can be divided into five stages, and two strong and continuous seismic reflections are observed in beach-bar seismic section.

4.2. Distribution Pattern of Beach-Bar Sand Bodies

The beach-bars developed in LST within Mbr2 in the WZ12-2 area of the Weixinan sag and can be further divided into five parasequences (Figure 8). Five stages of sand bodies are identified according to the five parasequences. From bottom to top, the percentage of sand decreases and the mud color becomes darker, indicating a rising lake level and a trend of retrogradational packages. The same phenomenon was also reported in beach-bar syndeposition in the Boxing and Banqiao sags within the Bohai Bay Basin [2,4,14,37]. The five stages of beach-bar sand bodies gradually retrograde towards the uplift (Figure 9).

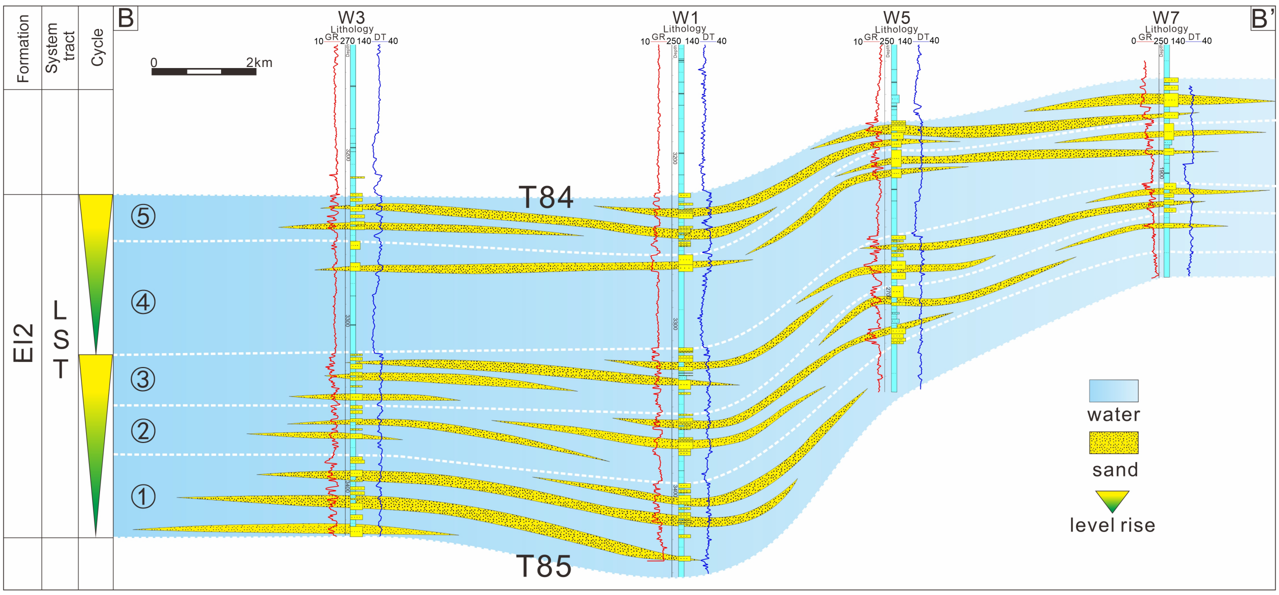

Figure 9. Sequence stratigraphic correlation section of beach-bar sand bodies of Mbr2 stage in the Weixinan sag. The five sand bodies in the LST show an obvious retrogradation upward.

Sand thickness contour maps were constructed to depict the distribution regularity of the five stages of beach-bar sand bodies in the WZ12-2 area of the Weixinan sag (Figure 10).

The shapes of five sand thickness contour maps vary with different depocenters. Sand ① has three depocenters, which are located near wells W3, W15 and W5. The directions of the long axis are northeast. Sand ② also has three depocenters near wells W5, W12 and W16. The long axis direction of two depocenters is northeast, and that of the third is north. Sand ③ has two depocenters in the vicinity of wells W13 and W5 with long axis directions oriented northeast. Compared with sand ③, sand ④ has one long axis direction oriented NNW. Sand ⑤, again, has three depocenters, but the long axes of the three depocenters change NNW and west-east. Although the long axis directions of the depocenters differ in each stage, the long axis direction of the whole beach-bar sand body remains to be northeast, which is constrained by the uplift geomorphology of Fault III in the northwest and the Qixi uplift in the northeast (Figure 11). Among these five stages of sands, the thickness of sand ③ is greatest, and the distribution area of sand ② is broadest. The distribution of the five stages of sands also shows retrogradation towards the uplift from sand ① to sand ⑤ (Figure 9). Additionally, changes in the depocenters, which are closely related to shoreline trajectory in the lake environment, show landward trend as transgression.

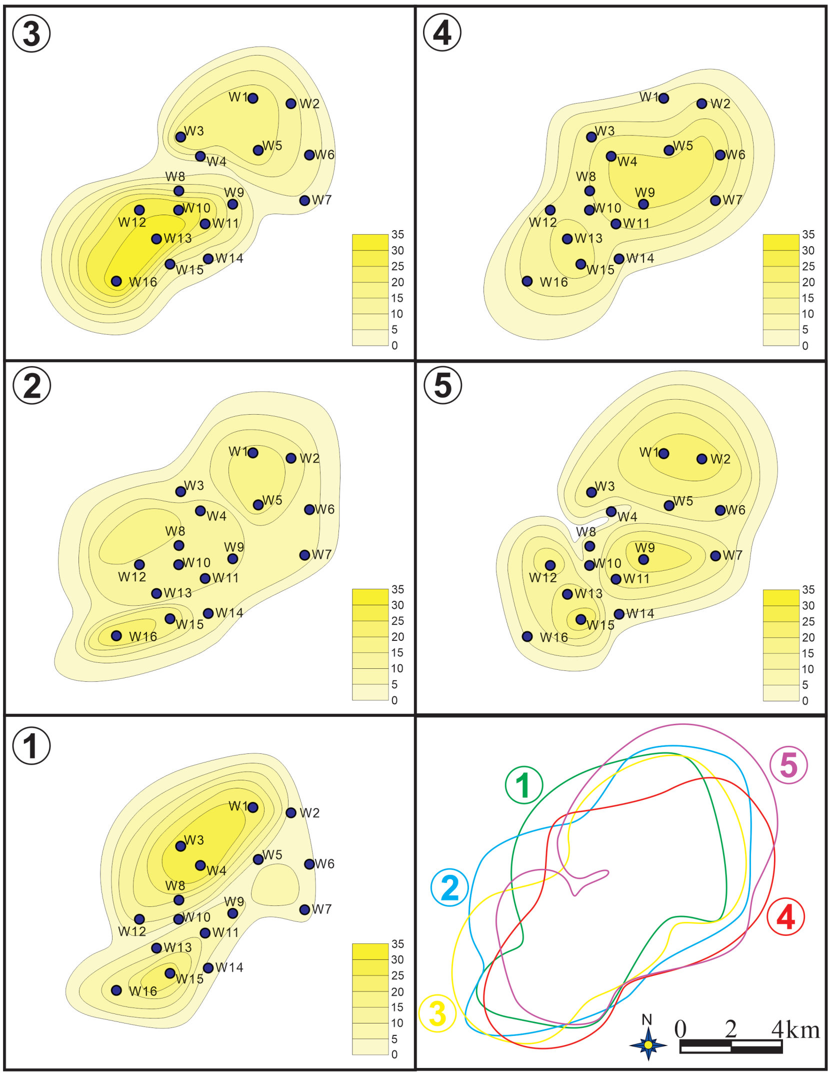

Figure 10. Isopach maps of sandstone thickness and distributions of the five stage sands in the LST of Mbr2 stage in the Weixinan sag. Note that the thickness of sand ③ is greatest, and the distribution area of sand ② is largest. Horizontal distribution of five stage sands also show a retrograding trend towards the uplift. The numbers ①–⑤ indicate the five stage sands in the LST of Mbr2 stage in the Weixinan sag from the bottom to top.

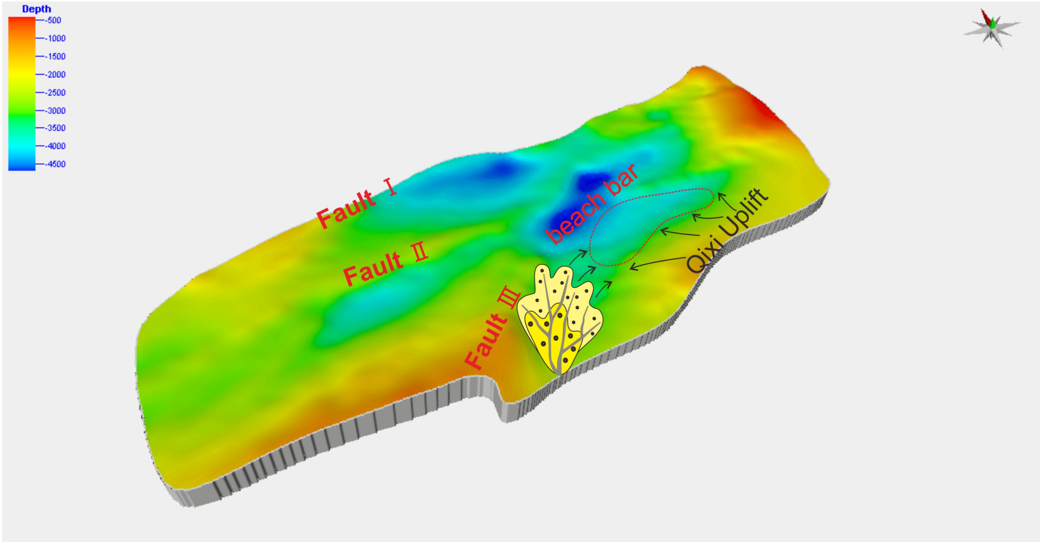

Figure 11. Paleotopography of depositional stage of Mbr2 showing the sediment provenance from the fan deltaic front and the Qixi uplift.

5. Discussion

5.1. Formation Mechanism

Comparing the HST and TST of the Mbr2 stage in the Weixinan sag, large-scale thick beach-bar sand bodies developed during the LST period. The formation of well-developed beach-bar sand bodies in the LST stage in the Weixinan sag was controlled by the paleotopography, hydrodynamic environment, sediment provenance and lake level variation.

5.1.1. Paleotopography

Beach-bars usually form in the early rifting or fault-depression transitional stage, during which tectonic movements is relatively stable [38]. Tectonic movements are closely related to paleotopography. Paleotopography is one of the most crucial factors controlling sedimentation [2,39–42]. Beach-bars may develop on large-scale gentle slopes of basins by studying the modern beach-bars in a faulted lacustrine basin [5]. It has been proposed that beach-bars may be well-developed on gentle slopes of lacustrine basins [2,4]. The favorable places for beach-bar deposition are subaqueous low uplifts, the flanks of nose structures and structural slope-break zones [43]. In this study, the beach-bar sand bodies that formed in the LST stage of Mbr2 in the WZ 12-2 area are situated on the southern slope of the Southeast Slope Belt, where a nose structure formed [28] and the slope angle was less than 1.2° (Figure 11) [23]. Therefore, the paleotopography in the WZ 12-2 area of the Weixinan sag provided good formation conditions for lacustrine beach-bar deposits.

5.1.2. Hydrodynamic Environment

The hydrodynamic environment is an important factor in beach-bar sand body formation and distribution [2,44–46]. Sediments from onshore continental areas are strongly scoured and reformed by lake waves and finally form beach-bar sand reservoirs in the gentle slope zone [4,47,48]. Different from rip and tide currents in marine coastal zones, lake currents are not very strong, and the primary source of hydrodynamic forces is mainly from shore wind waves [49]. On the windward side of the basin, the water in the lake is dragged to move, and friction is generated by wind on the water surface, finally producing waves [4]. Numerous factors, e.g., wind direction, wind force, wind duration and fetch length, can affect wave actions. The directions of the prevailing modelled surface currents (upper 100 m) during the summer and winter monsoons in the Beibuwan Basin during the Mbr2 period were southwest and northeast, respectively [50,51]. Therefore, the waves moved back and forth between the southwest and the northeast. Thus, waves affected a broad area in the southern Southeast Slope Belt. In the northwest, the sands of the fan delta developed along the Fault III were scoured and reworked by lake waves. The waves transported the sands to the gentle slope area and formed beach-bar deposits. The hydrodynamic conditions during the LST stage of the Weixinan sag were relatively strong. The paleowater water depth during the LST stage of Mbr2 was relatively shallow. The paleowater depth of the northwestern footwall of Fault III was deeper than that of the southern Southeast Slope Belt. In general, the Weixinan sag in the Beibuwan Basin during the LST period had strong hydrodynamic conditions with shallow lake water, which laid a good foundation for beach-bar sand body deposition.

5.1.3. Sediment Provenance

It has been proposed that the sediment provenance for lacustrine beach-bar sand bodies may be fan or braided deltas [2,48,52]. During the Mbr2 period in the Weixinan sag, the main sediment sources for beach-bars were the northwestern fan delta and the southeastern Qixi uplift [23,28]. The northwestern fan deltaic sediments acted as a point source (Figure 11). Sand bodies from the deltaic front could have been scoured and reworked by wave currents, producing the five stages of retrograded beach-bar sand bodies. Meanwhile, the nose structure that developed in the Qixi uplift in the southeast served as a large linear source, generating a persistent and abundant sediment supply. The nose structure in the northern Qixi uplift had already been denuded since the Mbr3 period [53]. The denuded sediments were transported to the Weixinan sag and frequently reworked, scoured and redeposited by lake waves and currents.

The distribution range of the lacustrine clastic beach-bar sand reservoirs was significantly affected by the supply and position of the sediment provenance. As a point source, the fan deltaic front in the northwest provided relatively limited amounts of sediment to the Weixinan sag. The water depth of the fan delta was relatively deep, and most of the fan deltaic sand bodies were below the wave base. Only few deposits could be reworked by lake waves. Sediments from the fan delta could reach the locations of wells W15 and W16 (Figure 12), which were the southwestern part of the beach-bar sand reservoirs. However, the linear source, the Qixi uplift, provided large quantities of sediments to the southern of Weixinan sag (Figure 12). The water depth in the southern Weixinan sag was shallow. Sediments from the Qixi uplift were continuously reworked by lake waves and currents, so the Qixi uplift was the main sediment source for the WZ12-2 beach-bar sand reservoirs in the Weixinan sag.

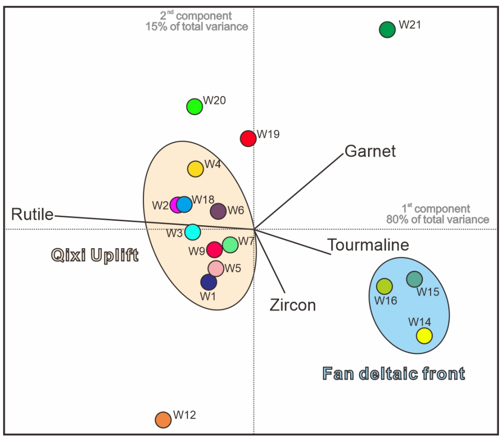

Figure 12. The rutile, garnet, tourmaline and zircon contents of beach-bar sandstones of Mbr2 stage in the Weixinan sag. The concentration of heavy minerals is controlled by sediment provenance. The beach-bar sediments were from the fan deltaic front and the Qixi uplift. The compositional biplot [54], drawn using CoDaPack software [55], displays multivariate observations (points) and variables (rays). The length of each ray is proportional to the variance of the corresponding element in the data set. If the angle between two rays is close to 0°, 90°, or 180°, then the corresponding elements are directly correlated, uncorrelated, or inversely correlated, respectively. Data for the biplot are provided in supplementary material.

5.1.4. Lake Level Oscillations

Lacustrine shallow littoral sand bodies usually spread parallel to shorelines, where lake level oscillations trigger back and forth movements of the shorelines, thus, controlling the shallow littoral sand body lateral distributions [2,4,53–59]. Previous research has proposed that repeated variations in lake level probably had a close relationship with Milankovitch cycles [46,60,61]. In this study, the lakeshore moved frequently and the water depth rose and fell rapidly during each parasequence set, most likely indicating the overfilled status of the lake [62,63]. Under the circumstances of low-relief paleogeomorphology, lake level changes can lead to the lateral migration of shorelines. The high-frequency variation of the lake level in the Weixinan sag contributed to the five stages of vertically stacked sands and to the formation of a wide lateral distribution of beach-bar sand reservoirs.

During the Mbr2 stage, lacustrine clastic beach-bar sand reservoirs formed during the LST period in the WZ12-2 area of the Weixinan sag. However, beach-bar formation was limited in the TST and HST stages. During the TST period, the quick rise in lake water level, together with the low sediment supply, led to starvation of the basin and formation of dark grey mudstones. In the LST stage, the lake level rise in the Weixinan sag was slow, and the source supply was limited [16], thus, the distribution range of beach-bars was largest in the LST period in the WZ12-2 area of the Weixinan sag.

5.2. Depositional Model of Lacustrine Beach-Bars

On the basis of the discussion above, a conceptual depositional model of lacustrine beach-bars in the WZ12-2 area of the Weixinan sag has been constructed to show the formation mechanism of beach-bar sand bodies (Figure 13). The deposition of beach-bar sand bodies in the WZ12-2 area of the Weixinan sag was favored by multiple factors: paleotopography, hydrodynamic environment, sediment provenance and lake level variation. During the deposition of Mbr2, the prevailing southwest summer and northeast winter monsoons and the paleotopography of the Weixinan sag, subjected the fan deltaic and gentle slope zones of the Southeast Slope Belt to lake wave impacts. Lake waves repeatedly washed and reworked the sand bodies sourced from the northwestern fan deltaic front and the southeastern Qixi uplift. Given the lake level oscillations, the shoreline migrated back and forth during each parasequence set. The frequent oscillations in lake level contributed to a wide distribution of beach-bars. The five stages of beach-bar sand bodies retrograded towards the shore with rising lake water.

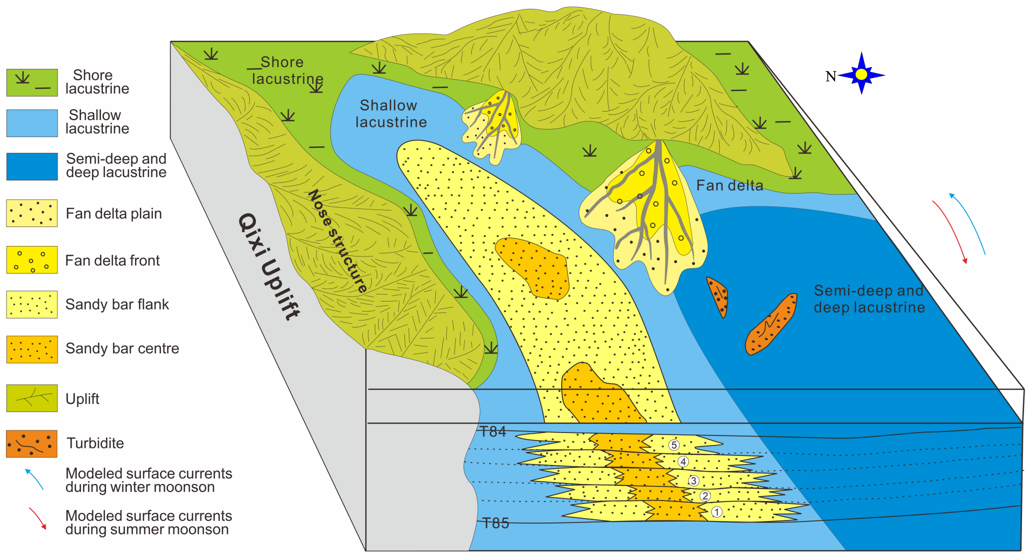

Figure 13. Depositional model for lacustrine beach-bar sand bodies in the LST stage of the Mbr2 period in the Weixinan sag.

In a sandy bar, the sandy bar center has thicker sandstones and higher porosity and permeability than the sandy bar flanks (Figure 4) and, thus, better reservoir quality. With thick source rocks at the bottom and good cap rock on top, a series of lithologic lenticular traps and sandstone pinch-out traps developed in the WZ12-2 area of the Weixinan sag. Oil exploration of lacustrine beach-bars in South China has rarely been reported [23,28,64], while much research on lacustrine beach-bars in East China have been published [2,4,11,14,65], especially in the Bohai Bay Basin. Important breakthroughs have been made in the exploration for oil in beach-bar deposits in the Bohai Bay Basin. The beach-bar sand bodies developed in South China and East China have similar characteristics. Beach-bars in both regions were located in gentle slope belts of a faulted basin during the middle stage of the Eocene, and controlled by the hydrodynamic environment, sediment source and lake level oscillations. Lacustrine beach-bar studies in East China basins can serve as a reference for further exploration of good lacustrine beach-bar sand body reservoirs in South China basins. The depositional model proposed in this study provides guidance for further prospecting and exploration of large-scale and thick beach-bar sand bodies during the LST periods in similar basins.

6. Conclusions

Beach-bar sand reservoirs formed in the Mbr2 of the Liushagang Fm. in the Weixinan sag. Five stages of beach-bar sand bodies developed vertically during the LST period of the Mbr2 sequence. The gently sloping paleotopography, strong hydrodynamic conditions in shallow water, abundant sediment sources and frequent lake water variations were the main factors that controlled beach-bar deposition. The northwestern fan deltaic front and the southeastern Qixi uplift were provenances for the beach-bar depositions. The beach-bar sand bodies that developed in the gently sloping belt within the Weixinan sag were subjected to strong hydrodynamic forces under shallow water conditions. Given these forces, together with repeated variations in lake level, the beach-bars retrograded vertically towards the shore and were distributed laterally over a large area. This study provides guidance for comparable beach-bar reservoirs in rift lacustrine basins with similar tectonic and depositional settings in the world.

Supplementary Materials: The following supporting information can be downloaded at: https://www.mdpi.com/article/10.3390/en15093391/s1, Table S1: The heavy mineral contents of beach-bar sandstones of Mbr2 stage in the Weixinan sag.

Author Contributions: Conceptualization, J.H. and H.W.; methodology, J.H.; software, J.H.; validation, E.L., S.C. and T.J.; formal analysis, S.C.; investigation, J.H.; resources, P.J.; data curation, T.J.; writing—original draft preparation, J.H.; writing—review and editing, T.J.; visualization, S.C.; supervision, H.W.; project administration, E.L.; funding acquisition, H.W. All authors have read and agreed to the published version of the manuscript.

Funding: This research was funded by the National Natural Science Foundation of China (U19B2007, 41972117, 41702121) and by the Major National Science and Technology Programs in the "Thirteenth Five-Year" Plan period (2016ZX05024-006-002).

Institutional Review Board Statement: Not applicable.

Informed Consent Statement: Not applicable.

Data Availability Statement: Not applicable.

Acknowledgments: We appreciate Zhanjiang Branch Company of China Offshore Oil Corporation for providing the data and permission to publish this paper. We are also very grateful to the reviewers and editors for their contributions to improving this paper.

Conflicts of Interest: The authors declared that they have no conflict of interest to this work. We declare that we do not have any commercial or associative interest that represents a conflict of interest in connection with the work submitted.

References

1. Basilici, G. Sedimentary facies in an extensional and deep-lacustrine depositional system: The Pliocene Tiberino Basin, Central Italy. *Sediment. Geol.* **1997**, *109*, 73–94. [CrossRef]
2. Jiang, Z.; Liu, H.; Zhang, S.; Su, X.; Jiang, Z. Sedimentary characteristics of large-scale lacustrine beach-bars and their formation in the Eocene Boxing Sag of Bohai Bay Basin, East China. *Sedimentology* **2011**, *58*, 1087–1112. [CrossRef]
3. Monroe, S. Late Oligocene-early Miocene facies and lacustrine sedimentation, upper Ruby River basin, Southwestern Montana. *J. Sediment. Res.* **1981**, *51*, 939–951.
4. Song, F.; Su, N.N.; Yang, S.C.; Yao, R.X.; Chu, S.M. Sedimentary characteristics of thick layer lacustrine beach-bars in the Cenozoic Banqiao Sag of the Bohai Bay Basin, East China. *J. Asian Earth Sci.* **2018**, *151*, 73–89. [CrossRef]
5. Soreghan, M.J.; Cohen, A.S. Textural and compositional variability across littoral segments of Lake Tanganyika: The effect of asymmetric basin structure on sedimentation in large rift lakes. *AAPG Bull.* **1996**, *80*, 382–409.
6. Zhu, X.M.; Xin, Q.L.; Zhang, J.R. Sedimentary characteristics and models of the beach-bar reservoirs in faulted down lacustrine basins. *Acta Sedimentol. Sin.* **1994**, *12*, 20–27, (In Chinese with English Abstract).
7. Otvos, E.G. Beach ridges definitions and significance. *Geomorphology* **2000**, *32*, 83–108. [CrossRef]
8. Tamura, T. Beach riges and prograded beach deposits as palaeoenvironment records. *Earth-Sci. Rev.* **2012**, *144*, 279–297. [CrossRef]
9. Reid, I.; Frostick, L.E. Beach orientation, bar morphology and the concentration of metalliferous placer deposits: A case study, Lake Turkana, N Kenya. *J. Geol. Soc.* **1985**, *142*, 837–848. [CrossRef]
10. Williamson, C.R.; Picard, M.D. Petrology of carbonate rocks of the Green River Formation (Eocene). *J. Sediment. Res.* **1974**, *44*, 738–759.
11. Deng, H.; Xiao, Y.; Ma, L.; Jiang, Z. Genetic type, distribution patterns and controlling factors of beach and bars in the second member of Shahejie Formation in the dawanbei sag, Bohai Bay, China. *Geol. J.* **2011**, *46*, 380–389.
12. Gao, X.; Deng, H.; Lin, H. Stratigraphic controls on the evolution and distribution of lacustrine beach and bar Sands-Bohai Bay basin in China. *Manuf. Eng. Environ. Eng.* **2014**, *84*, 1513–1519.
13. Goulart, E.S.; Calliari, L.J. Medium-term morphodynamic behavior of a multiple sand bar beach. *J. Coast. Res.* **2013**, *65*, 1774–1779. [CrossRef]
14. Wang, J.; Cao, Y.; Liu, K.; Wang, X.; Xiao, J.; Xie, N. Mass transfer between mudstone-sandstone interbeds during diagenesis as revealed from the type and distribution of carbonate cements in the Eocene beach-bar sandstones, Bohai Bay Basin. *Mar. Petrol. Geol.* **2019**, *110*, 21–34. [CrossRef]
15. Zhao, Y.; Wang, H.; Yan, D.; Jiang, P.; Chen, S.; Zhou, J.; Zhao, Y. Sedimentary characteristics and model of gravity flows in the Eocene Liushagang Formation in Weixi'nan depression, South China Sea. *J. Petrol. Sci. Eng.* **2020**, *190*, 107082. [CrossRef]
16. Cao, L.; Zhang, Z.; Li, H.; Zhong, N.; Xiao, L.; Jin, X.; Li, H. Mechanism for the enrichment of organic matter in the Liushagang Formation of the Weixinan Sag, Beibuwan Basin, China. *Mar. Petrol. Geol.* **2020**, *122*, 104649. [CrossRef]
17. Huang, B.J.; Tian, H.; Wilkins, R.W.T.; Xiao, X.M.; Li, L. Geochemical characteristics, palaeoenvironment and formation modelof Eocene organic-rich shales in the Beibuwan Basin, South China Sea. *Mar. Petrol. Geol.* **2013**, *48*, 77–89. [CrossRef]
18. Xie, J.Y.; Li, J.; Mai, W.; Zhang, H.L.; Cai, K.L.; Liu, X.Y. Palynofloras and age of the Liushagang and Weizhou formations in the Beibuwan Basin, south China sea. *Acta Palaeontol. Sin.* **2012**, *51*, 385–394.
19. Xu, X.D.; Wang, B.W.; Li, X.H.; Liu, M.Q.; Zhang, Y.Z.; Hang, B.J. Oil sources of concealed reservoirs in Liushagang formations of the Weixi'nan sag and accumulation feature, Beibuwan Basin. *Nat. Gas Geosci.* **2012**, *23*, 92–98.
20. Zhou, X.; Gao, G.; Lü, X.; Zhao, L.; Dong, Y.; Xu, X.; Gan, J. Petroleum source and accumulation of WZ12 oils in the Weixi'nan sag, South China Sea, China. *J. Petrol. Sci. Eng.* **2019**, *177*, 681–698. [CrossRef]
21. Huang, B.J.; Xiao, X.M.; Cai, D.S.; Wilkins, R.W.T.; Liu, M.Q. Oil families and their source rocks in the weixinan sub-basin, Beibuwan basin, South China Sea. *Org. Geochem.* **2011**, *42*, 134–145. [CrossRef]
22. Gao, G.; Zhou, X.X.; Dong, Y. *Detailed research of petroleum generation and accumulation in Liushagang Formation of Weixi'nan Sag, Beibuwan Basin (Internal Report of Zhanjiang Branch of the China National Offshore Oil Company)*; China National Offshore Oil Company: Zhanjiang, China, 2014.
23. Luo, B.H.; He, J.; Jiang, P.; Qin, C.Y.; Yang, X.B.; Lu, J.; Zhao, Y.P. Sedimentary Characteristics of Lacustrine Beach-bars and Their Formation of the Second Member of Liushagang Formation in the Paleogene Weixinan Sag of Beibuwan Gulf Basin, Northern South China Sea. *Geol. Sci. Technol. Inf.* **2019**, *38*, 186–196, (In Chinses with English Abstract).
24. He, J.; Wang, H.; Tang, J.; Shangguan, Y.; Yang, X.; Gong, Y.; Zhao, R.; Zhou, X. Evaluation of lacustrine mudstone top sealing capacity in the Lenghu-5 area, Qaidam Basin, Tibetan Plateau. *J. Petrol. Sci. Eng.* **2020**, *188*, 106973. [CrossRef]
25. Gao, Z.; Yang, X.; Hu, C.; Wei, L.; Jiang, Z.; Yang, S.; Fan, Y.; Xue, Z.; Yu, H. Characterizing the pore structure of low permeability Eocene Liushagang Formation reservoir rocks from Beibuwan Basin in northern South China Sea. *Mar. Petrol. Geol.* **2019**, *99*, 107–121.
26. Hao, F.; Zhou, X.H.; Zhu, Y.M.; Bao, X.H.; Yang, Y.Y. Mechanisms for oil depletion and enrichment on the Shijiutuo uplift, Bohai Bay Basin, China. *AAPG Bull.* **2009**, *93*, 1015–1037. [CrossRef]
27. Wang, J.; Cao, Y.C.; Li, J.L. Sequence structure and non-structural traps of the Paleogene in the Weixi'nan Sag, Beibuwan Basin. *Pet. Explor. Dev.* **2012**, *39*, 325–334. [CrossRef]

28. Wang, J.; Cao, Y.C.; Li, J.L.; Yue, Y.X. Distribution of beach-bar sandbodies of the second member of Liushagang Formation of Paleogene of south slope in Weixinan Depression, Beibuwan Basin. *Acta Sedimentol. Sin.* **2013**, *31*, 536–544, (In Chinese with English Abstract).
29. Liu, P.; Xia, B.; Tang, Z.Q.; Wang, X.G.; Zhang, Y. Fluid inclusions in reservoirs of Weixinan Sag, Beibuwan Basin. *Petrol. Explor. Dev.* **2008**, *35*, 164–200. [CrossRef]
30. Liu, Y.; Wu, Z.; Liu, L.; Yan, S.; Hu, L.; Ping, M.; Zhang, M. Cenozoic structure and tectonics of North subbasins in Beibu Gulf Basin, northern South China Sea. *Tectonophysics* **2021**, *812*, 228912. [CrossRef]
31. Liu, E.; Wang, H.; Li, Y.; Zhou, W.; Leonard, N.D.; Lin, Z.; Ma, Q. Sedimentary characteristics and tectonic setting of sublacustrine fans in a half-graben rift depression, Beibuwan Basin, South China Sea. *Mar. Petrol. Geol.* **2014**, *52*, 9–21. [CrossRef]
32. Vail, P.R.; Audemard, F.; Bowman, S.A. The stratigraphic signatures of tectonics, eustasy and sedimentology—An overview. In *Cycles and Events in Stratigraphy*; Springer: Berlin/Heidelberg, Germany, 1991; Volume 6, pp. 7–659.
33. Scherer, C.M.; Lavina, E.L.; Dias Filho, D.C.; Oliveira, F.M.; Bongiolo, D.E.; Aguiar, E.S. Stratigraphy and facies architecture of the fluvial-Aeolian-lacustrine Sergi Formation (Upper Jurassic), Reconcavo Basin, Brazil. *Sediment. Geol.* **2007**, *194*, 169–193. [CrossRef]
34. Garzanti, E. Petrographic classification of sand and sandstone. *Earth-Sci. Rev.* **2019**, *192*, 545–563. [CrossRef]
35. Schwartz, R.K. Bedform, texture, and longshore bar development in response to combined storm wave and current dynamics in a nearshore helical flow system. *J. Coast. Res.* **2012**, *28*, 1512–1535. [CrossRef]
36. Short, A.D. Multiple offshore bars and standing waves. *J. Geophys. Res.* **1975**, *80*, 3838–3840. [CrossRef]
37. Yang, Y.Q.; Qiu, L.W.; Jiang, Z.X.; Yin, X.L. A depositional pattern of beach bar in continental rift lake basins: A case study on the upper part of the fourth member of the Shahejie Formation in the Dongying Sag. *Acta Petrol. Sin.* **2011**, *32*, 417–423.
38. Lin, H.X.; Deng, H.W.; Qin, Y.Q.; Gao, X.P.; Long, G.Q.; Zhao, N.; Yan, H.; Pan, F.Y.; Di, Y.X. Control of sequence stratigraphic evolution on the distribution and hydrocarbon accumulation of beach and bar reservoirs. *Petrol. Expl. Dev.* **2010**, *37*, 680–689, (In Chinese with English Abstract).
39. Distefano, S.; Gamberi, F.; Baldassini, N.; Di Stefano, A. Neogene stratigraphic evolution of a tectonically controlled continental shelf: The example of the Lampedusa island. *Ital. J. Geosci.* **2019**, *138*, 418–431. [CrossRef]
40. Guo, S. The influence of the pre-existing topography on the depositionary systems, the development of the Lower Jurassic reservoirs and hydrocarbon accumulation in Central Western Ordos Basin. *J. Petrol. Sci. Eng.* **2010**, *75*, 129–134. [CrossRef]
41. Paul, J.M.; Peter, M.I.; Dale, A.L. Use of micromorphology for palaeoenvironmental interpretation of complex alluvial palaeosols: An example from the MillCreek Formation (Albian), southwestern Alberta, Canada. *Palaeogeogr. Palaeoclimatol. Palaeoecol.* **1998**, *143*, 87–110.
42. Zhu, X.M.; Liu, Q.H.; Ge, J.W.; Dong, Y.L.; Zhu, S.F.; Tan, M.X.; Yang, Y. Reconstruction of sediment-dispersal patterns using seismic sedimentology in the southeastern Zhanhua Sag, Bohai Bay Basin, China. *J. Petrol. Sci. Eng.* **2019**, *182*, 106335.
43. Jiang, Z.X.; Wang, J.H.; Zhang, Y.F. Advances in beach-bar research: A review. *J. Palaeogeogr.* **2015**, *17*, 427–440, (In Chinese with English Abstract).
44. Graham, J.P. Revised stratigraphy, depositional systems, and hydrocarbon exploration potential for the lower Cretaceous muddy sandstone. Northern Denver Basin. *AAPG Bull.* **2000**, *84*, 183–209.
45. Wang, J.; Xu, S.; Yu, J.; Han, W.; Cui, H.; Zhai, Y. Prediction of beach-bar sand reservoirs using waveform analysis: A case study on Es4s in the west area of the Dongying sag. *Earth Sci. J. Chin. Univ. Geosci.* **2008**, *33*, 627–633.
46. Zhang, Y.; Hu, C.; Wang, M.; Ma, M.; Wang, X.; Jiang, Z. A quantitative sedimentary model for the modern lacustrine beach bar (Qinghai Lake, Northwest China). *J. Paleolimnol.* **2018**, *59*, 279–296. [CrossRef]
47. Gao, Y.F.; Peng, S.P.; He, H.; Kong, W. Reservoir characters and evaluation of the Tertiary clastic sediments in the Northern Qaidam basin, Northwest. *China. Petrol. Expl. Dev.* **2003**, *30*, 40–42.
48. Keighley, D.; Flint, S.; Howell, J.; Moscarliello, A. Sequence stratigraphy in lacustrine basin: A model for part of the Green River Formation (Eocene), Southwest Uinta Basin, Utah, USA. *J. Sediment. Petrol.* **2003**, *73*, 987–1006. [CrossRef]
49. Cook, D.O. The occurrence and geologic work of rip currents of southern California. *Mar. Geol.* **1970**, *9*, 173–186. [CrossRef]
50. Huang, E.; Tian, J.; Steinke, S. Millennial-scale dynamics of the winter cold tongue in the southern South China Sea over the past 26ka and the East Asian winter monsoon. *Quat. Res.* **2011**, *75*, 196–204. [CrossRef]
51. Schroeder, A.; Wiesner, M.G.; Liu, Z.F. Fluxes of clay minerals in the South China Sea. *Earth Planet. Sci. Lett.* **2015**, *430*, 30–42. [CrossRef]
52. Zhu, X.M.; Zhong, D.K.; Yuan, X.J.; Zhang, H.L.; Zhu, S.F.; Sun, H.T.; Gao, Z.Y.; Xian, B.Z. Development of sedimentary geology of petroliferous basins in China. *Petrol. Expl. Dev.* **2016**, *43*, 890–901. [CrossRef]
53. Xie, N.; Cao, Y.C.; Wang, J.; Jin, J.H.; Zhang, W.J.; Zhong, Z.H. Diagenesis and its control on physical property of the reservoirs in the 3rd member of the Paleogene Liushagang Formation in Weixinan Depression, Beibuwan Basin. *Nat. Gas Geosci.* **2019**, *30*, 1743–1754, (In Chinese with English Abstract).
54. Gabriel, K.R. The biplot graphic display of matrices with application to principal component analysis. *Biometrika* **1971**, *58*, 453–467. [CrossRef]
55. Comas Cufí, M.; Thió Fernández de Henestrosa, S. CoDaPack 2.0: A stand-alone, multi-platform compositional software. In *CoDAWork'11: 4th International Workshop on Compositional Data Analysis, Sant Feliu De Guíxols*; CoDAWork'11: Girona, Spain, 2011.

56. Distefano, S.; Gamberi, F.; Baldassini, N.; Di Stefano, A. Quaternary evolution of coastal plain in response to sea-level changes: Example from south-east Sicily (Southern Italy). *Water* **2021**, *13*, 1524. [CrossRef]
57. Carroll, A.R.; Bohacs, K.M. Lake type control on hydrocarbon source potential in nonmarine basins. *AAPG Bull.* **2001**, *85*, 1033–1053.
58. Hou, F.H.; Jiang, Y.Q.; Fang, S.X.; Guo, G.A.; Yang, J.L. Sedimentary model of sandstone in second and fourth members of Xiangxi formation in the upper Triassic of Sichuan basin. *Acta Petrol. Sin.* **2005**, *26*, 30–37.
59. Yuretich, R.F.; Hickey, L.J.; Gregson, B.P.; Hsia, Y.L. Lacustrine deposits in the Paleocene Fort Union Formation, Northern Bighorn Basin. Montana. *J. Sediment. Petrol.* **1984**, *54*, 836–852.
60. Xia, S.; Lin, C.; Du, X.; Jia, D.; Ahmad, N.; Zhang, Z.; Gao, L.; Zhu, Y. Correspondences among lacustrine fluctuations, climate changes and the Milankovitch cycles in the Paleogene through tracking onlap points and correlating palaeontology in Liaozhong Depression, Bohai Bay Basin, NE China. *Geol. J.* **2020**, *55*, 6527–6543. [CrossRef]
61. Milankovitch, M. Kanon der Erdbestrahlung und seine Anwendung auf das Eiszeitenproblem. *Beogr. Königlich Serbische Akad.* **1941**, *32*, 633.
62. Bohacs, K.M.; Carroll, A.R.; Neal, J.E.; Mankiewicz, P.J. Lake-Basin type, source potential, and hydrocarbon character: An integrated sequence-stratigraphic-geochemical framework. In *Lake Basins through Space and Time*; Gierlowski-Kordesch, E.H., Kelts, K.R., Eds.; American Association of Petroleum Geologists: Tulsa, OK, USA, 2000; Volume 46, pp. 3–34.
63. Cong, F.; Zhu, F.; Cai, Z.; Chen, H.; Li, J.; Wang, Y.; Wang, L. Orbitally forced glacio-eustatic origin of third-order sequences and parasequences in the Middle Permian Maokou Formation, South China. *Mar. Petrol. Geol.* **2019**, *99*, 237–251. [CrossRef]
64. Liu, Q.; Zhu, H.; Shu, Y.; Zhu, X.; Yang, X.; Chen, L.; Tan, M.; Geng, M. Provenance identification and sedimentary analysis of the beach and bar systems in the Palaeogene of the Enping Sag, Pearl River Mouth Basin, South China Sea. *Mar. Petrol. Geol.* **2016**, *70*, 251–272. [CrossRef]
65. Wang, Y.; Yang, S.; Zhang, Y.; Lu, Y.; Wang, Y.; Zhao, Y. Investigation of pore structure and reservoir quality of Eocene beach-bar sandstones in Dongying Depression, Bohai Bay Basin, East China. *J. Petrol. Sci. Eng.* **2020**, *189*, 106854. [CrossRef]